Polarization and Interference

Nolan Tremelling

October 26, 2023

Abstract

An experiment to investigate the wave mechanics of polarization and interference. Conducted with light, but generalize to other waves, as well.

1 Introduction

While there exists a wide range of wave phenomena in nature, two classifications of waves emerge: the longitudinal wave, and the transverse wave. Longitudinal waves vibrate parallel to the direction of wave propagation while transverse waves vibrate perpendicular to the direction of propagation.

Transverse waves can be subject to polarization, or the oscillation along only one axis within the plan perpendicular to the direction of propagation. An example of a transverse wave that can be polarized is light, where the polarization state of light is in reference to the vibration axis of the electric field due to the inherent electromagnetic radiation that light exhibits. Light from a source such as a flame is typically unpolarized—the electric field is oscillating at random with respect to the plane perpendicular to the direction of propagation. Through filtering, such as that shown in Figure 1, we subject unpolarized light to a polarization filter, causing only the component of the electric field perpendicular to the absorption material's (typically a polymer film) long axes to be transmitted. The resulting direction perpendicular to the molecular chains is the transmission axis.

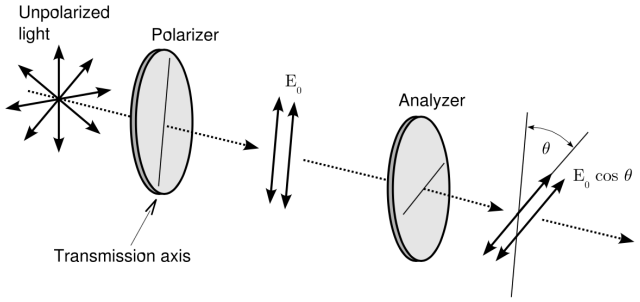

Figure 1: Creation and detection of polarized light.

Being subject to polarization through a filter, the resulting wave can be analyzed through a second filter with a transmission axis oriented at an angle θ with respect to the first filter. This allows for the component of $\vec{E_o}$ parallel to its transmission axis, $E_0 cos(\theta)$ to be selected. Malus'

Law then gives the intensity of light after it passes through the analyzer as given in Equation 1, where $I_0 = |\vec{E}_0|^2$.

$$I = I_0 cos^2\theta \tag{1}$$

Waves additionally have a property of superimposition. When two waves encounter each other in a medium, the resultant wave is the algebraic sum of the two individual waves. Depending on the phase and magnitude of these waves, either constructive or destructive interference is observed, where the resultant wave has a peak greater than or less than either individual wave, respectively. Constructive interference results in an increase in the intensity of light, while destructive interference results in a decrease in intensity.

First clearly demonstrated by Thomas Young in 1801, a light beam was passed through two narrow slits resulting in a wavelike interference, forming a pattern of bright and dark spots. This experiment illustrated the geometric underpinnings of the resulting interference pattern. From a fairly elementary analysis, given that there is a difference in path length $\Delta l = dsin\theta$, the maxima and the minima of the interference pattern are found to occur when the two waves are perfectly in phase, that is $\theta = 0°$ and out of phase, $\theta = 180°$, respectively. The maximum will then occur at integer multiples of Δl, such that $\Delta l = m\lambda, m = 0, \pm1, \pm2, \ldots$. The minimum occurs at half-integer multiples of Δl, such that $\Delta l = (m + \frac{1}{2})\lambda, m = 0, \pm1, \pm2, \ldots$. Through taking a small angle approximation, it is found that the position of the m^{th} maximum is $sin\theta_m \approx tan\theta_m \approx \frac{x_m}{D}$.

he observed interference pattern will not just exhibit a straightforward interference pattern. While the double-slit diffraction pattern exhibits periodicity, it also displays prominent features. This nuanced pattern arises due to a blend of interference effects inherent to the double-slit experiment as well as the diffraction effect originating from each individual slit. This intensity for the single-slit pattern can be mathematically represented as:

$$I = I_0 \left(\frac{\sin\left(\pi a \sin\theta/\lambda\right)}{\pi a \sin\theta/\lambda} \right)^2$$

Here, a signifies the width of the slit. It becomes evident that the minima for the single-slit interference pattern emerge when:

$$\frac{\pi a \sin\theta}{\lambda} = n\pi \quad (n = \pm1, \pm2, \ldots)$$

Which can be further simplified to:

$$\sin\theta_n = \frac{n\lambda}{a}$$

Applying the aforementioned small angle approximation, we can translate the above relationship into the positions x_n of the single-slit minima on the observation screen as:

$$x_n = \left(\frac{\lambda D}{a} \right) n$$

In summary, the interplay of interference from both slits combined with the diffraction effect of individual slits shapes the intricate intensity pattern observed in the double-slit experiment.

2 Method

A range of sophisticated optical equipment is employed in this experiment. Central to this setup is the Light Sensor paired with a Rotary Motion Sensor (RMS). The Light Sensor detects and measures the total power of the incident light, while the RMS, mounted on a linear translator, gauges and reports the current transverse position, allowing for adjustments transverse to the optical bench. Another pivotal component is the Double/Single Slit Disk, housing various slits that can be interchanged by rotating the disk. Additionally, a polarizer equipped with RMS is utilized, serving to polarize unpolarized light and potentially function as an analyzer, with its rotation angle measurable via the RMS. The experiment is performed in two distinct parts. Initially, the polarizer with RMS is harnessed in conjunction with a laser light source to validate Malus' Law. Then, the polarizer is disengaged, the slits are installed, and both double and single-slit diffraction patterns of laser light are observed. The choice of the laser is strategic, given its capability to emit intense, coherent light of a singular wavelength, ensuring all light waves remain in phase.

3 Results and Discussion

3.1 Polarization

As detailed above, the Polarization Analyzer with the Rotary Motion Sensor (RMS) is placed between the laser and the Light Sensor. The polarizer is than rotated 360 degrees (one revolution) and measurements are recorded. In Figure 2 three trials are detailed. To accurately analyze these, we must normalize their phase and ensure that θ_0 is subtracted from the measured angles. The normalized graph is shown in Figure 3. Finally, we evenly sample a distribution of 20 points and plot the associated error with each point. This is shown in Figure 4. From this, we see it is found that the maximum intensity, I_0, is found at the normalized angle $\theta = 0°$ with a value of 2782.16 ± 21.54. Further, it is found that only one point lies outside of 1σ, with no points lying outside of $2\sigma, 3\sigma$. Figure **??** tests Malus' Law, plotting I/I_0 against $cos^2\theta$, where θ. As expected, this produces a straight line with a slope of 0.9801 ± 0.0125 and an intercept of 0.0190 ± 0.0080.

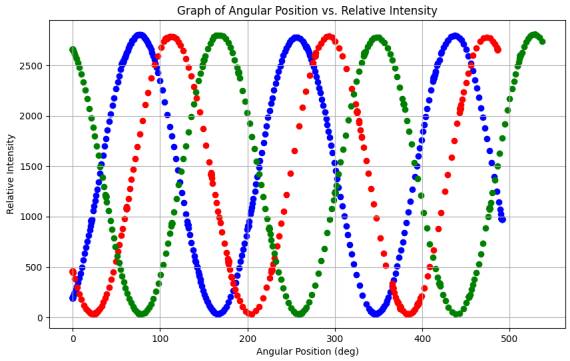

Figure 2: Raw data from three trials reveals that the measurements are out of phase.

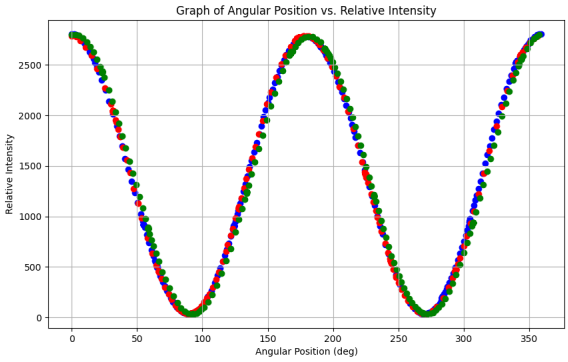

Figure 3: Phase and angle normalized plots for three trials.

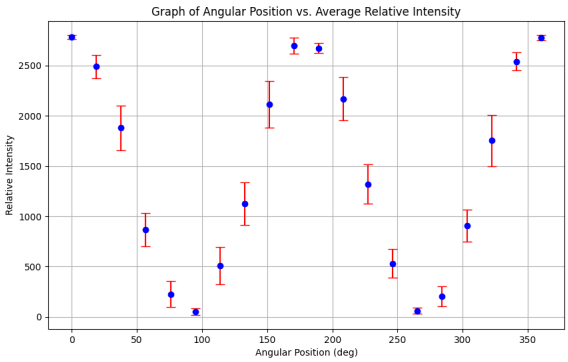

Figure 4: Evenly sampled plot with associated error.

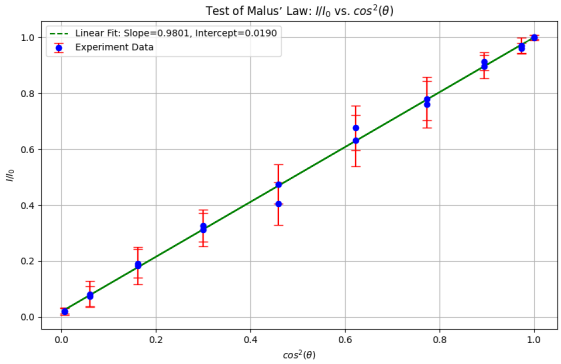

Figure 5: A plot of Malus' Law, demonstrating $I/I_0 vs. cos^2\theta$

We find that there is an ambient noise of 51.38 ± 32.50. In a perfect environment, we expect an absence of noise, however due to ambient light, and light from sources such as cell phones, computers, etc. it becomes exceedingly difficult to ensure that there is no other light in the room. Our signal to noise ratio is found to be 54.15 ± 34.25, implying that the signal is approximately 54 times the strength of the noise. This shows that a strong signal was captured, however further reduction of the ambient noise would likely improve this even more. The y-intercept here

corresponds to the intensity that remains even when the polarizer is perpendicular to the plane of polarization. Ideally, this value should be zero, since no light should pass through. However, due to the same ambient light sources, it is measured to be 0.0190 ± 0.0080. Using an incandescent bulb (or another broad spectrum light source) for the experiment would introduce variability due to the variation of emitted light, making results less distinct compared to a laser. The incoherent nature of the bulb's light could also increase noise levels in the measurements.

3.2 Double Slit Diffraction Pattern

The positions of the double slit diffraction maxima x_m are plotted against the order number m as seen in Figure 6. Through a least squares analysis, the slope of the data, which represents $\frac{\lambda L}{d}$, was found. Here, λ is the wavelength of the laser light, L is the distance between the slits and the screen, and d is the separation between the slits. Given the known values of L and d, the estimated wavelength λ was calculated as $\lambda = 242.9$nm. The obtained value differs from the expected value of 650nm for the red laser. This discrepancy likely arises due to experimental errors and precision of measurements, especially when the precision of the measurement tools is taken into consideration. Three fringes were observed during the experiment. The number of fringes visible depends on various factors including the coherence length of the light source, the alignment of the apparatus, and ambient lighting conditions. It should be possible to see more fringes by using a light source with a longer coherence length, ensuring precise alignment of the apparatus, and minimizing ambient light and other sources of interference. The precision of this measurement is limited by the accuracy of the measuring instrument, stability and alignment of the experimental setup, and external disturbances. The distance between the slits and the laser, or the slit-to-light sensor spacing, affects the fringe pattern's width and visibility. As this distance increases, the fringes spread out and become more distinct but decrease in intensity. Conversely, decreasing this distance makes the fringes closer together and harder to resolve but may increase their intensity.

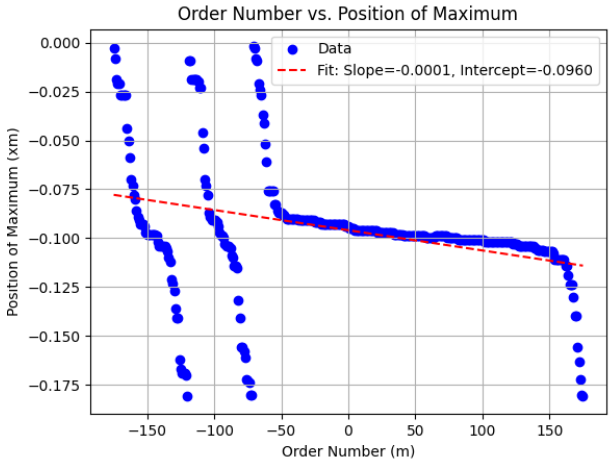

Figure 6: Order Number vs. Positions for M

3.3 Single Slit Envelope

A plot was constructed to showcase the relationship between the positions of diffraction maxima, denoted as x_n, and the order number n, which counts from the central maximum in either direction.

From this plot, a wavelength value of $\lambda = -0.0000005936\,\text{m}$ (equivalently, 593.6 nm) is obtained, and the slit width, represented by a, was estimated to be $0.000250\,\text{m}$ or $250\,\mu\text{m}$. This estimated slit width is equal to the nominal width specified on the experimental component, which is 0.04 mm. This reinforces a precision in both the experimental setup and the subsequent data analysis. Comparing the envelopes of the double and single slits, the prominence of the double slit envelope is indicative of the slit separation (d) being considerably larger than the slit width (a). If the slit width of the double slit, a, were to be altered, the diffraction pattern would experience corresponding changes. An increment in a would broaden the individual diffraction peaks, thus reducing the overall number of discernible peaks. On the other hand, a decrement in a would lead to the peaks becoming narrower, thereby amplifying the number of visible peaks. This modification in slit width would also have a perceptible effect on the overall visibility and contrast of the interference pattern.

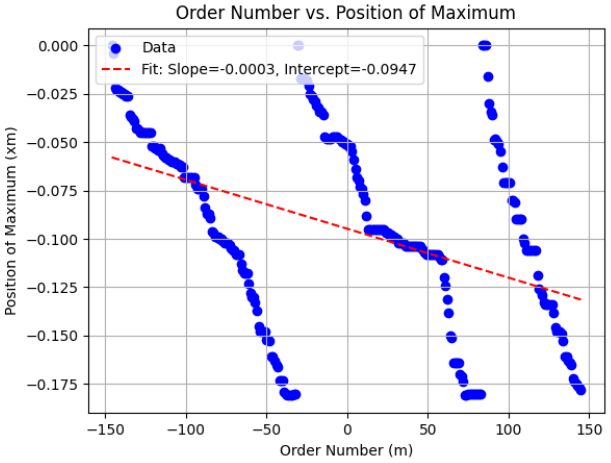

Figure 7: Order Number vs. Positions for N

4 Conclusion

This experiment successfully explored the wave mechanics of polarization and interference using light as the primary medium. Malus' Law was verified by subjecting unpolarized light to a polarization filter and subsequently analyzing it through another polarizer set at an angle θ. The data collected confirmed Malus' prediction for light intensity after passing through an analyzer, with minor discrepancies likely due to ambient light sources. The experimental setup also successfully demonstrated the double-slit interference and single-slit diffraction patterns, which are foundational experiments in wave physics. From the double-slit interference pattern, a laser light wavelength of 242.9nm was deduced, deviating from the expected 650nm for the red laser, suggesting potential experimental inaccuracies or measurement precision limitations. The single-slit experiment yielded a wavelength of 593.6nm, much closer to the anticipated value, and successfully determined the slit width to be 250µm, consistent with the specified component width. This suggests a high degree of precision in the experimental procedure and subsequent data analysis for the single-slit experiment. Overall, the findings underscore the intricate nature of wave mechanics and the importance of accurate experimental conditions in studying wave phenomena.